Reductive photocatalytic decolourization of an azo dye Reactive Black 5 using TiO$_2$: mechanism and role of reductive species

Bhaumik R. Shah[a], Upendra D. Patel[b,*]

[a]Civil Engineering Department, C.S. Patel Institute of Technology, Charotar University of Science & Technology, Gujarat, India, email: bhaumik_me@yahoo.com
[b]Civil Engineering Department, Faculty of Technology & Engineering, The M.S. University of Baroda, Gujarat, India, emails: patelupendra@gmail.com, udpatel-ced@msubaroda.ac.in

ABSTRACT

Photocatalytic oxidation of dyes using TiO$_2$ is amply studied; however, there are no reports demonstrating reductive photocatalytic decolourization of dyes and underlying mechanisms. We investigated photocatalytic reduction of Reactive Black 5 (RB5) dye using TiO$_2$ and UV light in the presence of various hole scavengers (HSs). Around 94% of 50 mg L^{-1} initial RB5 was decolourized in the presence of 2 mM oxalic acid (OA) and 0.5 g L^{-1} TiO$_2$, after 1 h irradiation at initial pH 2.8. OA yielded highest rate and extent of RB5 decolourization among all HS, probably due to superior hole-scavenging activity and capacity to produce reductive radicals. LC-MS analysis of decolourized RB5 sample revealed the presence of 2-((4-aminophenyl) sulphonyl) ethyl hydrogen sulphate, and 3,4,6-triamino-5-hydroxynaphthalene-2,7-disulphonic acid as end-products; indicating cleavage of azo bonds as a main mechanism of decolourization. The contribution of reducing species for reductive RB5 decolourization was found to be in the order of $e_{cb}^- > C_2O_4^{\bullet -}$ radical $> CO_2^{\bullet -}$ radical. The rates of RB5 decolourization, appearance and time point of highest accumulation of end-products, were greatly influenced by the initial pH, type and concentration of HS. TiO$_2$ exhibited excellent reusability and regenerability. Around 65% decolourization was obtained even after the fifth reuse. The regenerated TiO$_2$ exhibited photocatalytic activity almost similar to the fresh TiO$_2$.

Keywords: Photocatalytic decolourization; Reactive Black 5; Hole scavenger; Reductive species; Reusability

1. Introduction

Synthetic dyes comprise an important part of the textile industry effluents. Around 10%–15% of the dyes used in the process of dying is discharged with wastewater. The presence of the dyes in the effluents is a cause of great environmental concern. The coloured wastewater due to the presence of dye can block both sunlight penetration and oxygen dissolution, which are essential for aquatic life. Azo dye is the largest class of dyes used, accounting for more than about half of the textile dyestuff used today [1]. They have one or more azo bonds (N=N) with aromatic rings mostly substituted by sulphonic (SO$_3$H) groups. These complex aromatic conjugated structures make them resistant to degradation under normal environmental conditions.

Conventional biological processes are ineffective in treating the azo dyes due to lower biochemical oxygen demand/chemical oxygen demand ratio. Anaerobic biological treatment can decolourize azo dyes by cleaving azo bonds producing aromatic amines. These amines may be biodegraded aerobically [2]. However, it may be difficult to find suitable redox conditions and electron acceptors during anaerobic biodegradation of azo dyes. Physicochemical treatment such as adsorption, coagulation, and membrane separation, on the other hand, results in to mere phase separation of target compounds rather than their destruction. Moreover, physicochemical processes lead to the generation of secondary waste which needs further treatment.

* Corresponding author.

Advanced oxidation processes such as Fenton [3], photo-Fenton [4], ozonation [5] and electrochemical oxidation [6] that use a strong oxidizing species such as •OH radicals produced in-situ has been used by many researchers for dye decolourization. In recent years the application of heterogeneous photocatalysis, which uses a light source with a semiconductor material to initiate the photoreaction, has been extensively explored. Semiconductors such as TiO_2, ZnO, CdS, Bi_2O_3, ZrO_2 and iron oxides can be used as catalyst directly or with some modifications for photocatalysis process. The majority of research on the application of photocatalysis for air and water purification involves the use of TiO_2 due to its exceptional optical and electronic properties, chemical stability, nontoxicity and low cost [7,8].

Photocatalytic oxidation (PCO) and photocatalytic reduction (PCR) are two sides of a coin [9]. Irradiation of TiO_2 with UV light results in formation of electron-hole pair [Eq. (1)]. The hole reacts with adsorbed water or hydroxyl ion to form hydroxyl radical (•OH) which is responsible for oxidation of organic pollutants. On the other hand, the electron generated may be exploited for reductive decomposition of target compound. The photogenerated electron has a strong reducing potential (–0.5 to –1.5V vs SHE) [10].

$$TiO_2 + h_v \rightarrow e_{cb}^- + h_{vb}^+ \tag{1}$$

To obtain greater number of electrons for reduction process, holes must be filled with electrons obtained from sacrificial oxidation of other compounds to maintain electroneutrality. Such an organic compound is called a hole scavenger (HS, electron donor) which sacrifices itself by scavenging the holes. Dissolved aqueous oxygen is a known electron scavenger [11]. It can form superoxide radicals which can ultimately form hydroxyl radicals (•OH), thereby enhancing oxidation and adversely affecting the reduction process as number of electrons available for reduction would decrease. Thus, to prevent production of oxidative species, O_2 needs to be purged out before and during the reaction. In addition to electrons, other reductive species may also be generated depending on the type of HS, such as $C_2O_4^{\bullet-}$ and $CO_2^{\bullet-}$ radicals, which also contribute to reduction of target compounds.

Decolourization of azo dyes by PCO using TiO_2 [12–16] and synthesized photocatalysts [17] has been abundantly reported in the published literature. However, literature on PCR is scarce. Selection of suitable HS is very important for the success of PCR process. PCR using various organic HS such as oxalic acid (OA) [18–20], formic acid (FA) [9,11,21–24], sodium formate [11,25], sodium oxalate [18], methanol [22–23,25], ethanol [18,22], 2-propanol (IPA) [23], EDTA [23,26], acetic acid [22], salicylic acid [22], citric acid [23,27] and succinic acid [23] has been investigated for reduction of inorganic anions and cations such as nitrate [11,18,21,24], selenium (IV) [22–23], toxic metal ions such as cadmium (II) [25], copper (II) [23,27], nickel (II) [27], zinc (II) [27], lead (II) [27] and chromium (VI) [28–30]. However, limited reports are available demonstrating PCR for degradation of organic pollutants such as dyes. Yin et al. [9] used PCR for dechlorination of pentachlorophenol; Wang et al. [19] for perfluorooctanoic acid (PFOA) and Guo et al. [31] for degradation of tetrabromobisphenol.

Thus, the objectives of the study were to demonstrate PCR of RB5 as a model azo dye and delineate the mechanism of decolourization. Since HSs play crucial role in PCR, the type and concentration of HS on PCR of RB5 have also been studied. Yet another objective of the study was to determine the contribution of various reductive species to RB5 decolourization. Commercially available P25 has been selected as catalyst instead of a lab synthesized catalyst; to ascertain the reproducibility of results. Reductive photocatalytic decolourization of RB5 and the role played by reductive species, depicted in the study, is not yet reported to the best of our knowledge. RB5 is selected as a model compound since it makes the largest fraction of reactive dyes produced in India [32].

Table S1 lists some general information about RB5. Table S2 and Fig. S1 show physicochemical and morphological properties of TiO_2.

2. Experimental

2.1. Chemicals

The Reactive Black 5 (RB5, $C_{26}H_{21}N_5Na_4O_{19}S_6$) dye (99% purity) was supplied by a local dye industry (Astron Chemicals, Ahmedabad). TiO_2 (P25) (>99.5%) having weight ratio of anatase to rutile phases as 80/20 was supplied by Evonik (formerly known as Degussa) as a free sample. Formic acid (HCOOH, 98%), OA ($H_2C_2O_4.2H_2O$), Ferric chloride ($FeCl_3$) and potassium oxalate supplied by Merck, India, were of analytical standard (Guaranteed Reagents). HPLC grade methanol (CH_3OH) and 2-propanol (C_3H_8O, AR grade) were supplied by Finar, India. All the solutions were prepared using distilled water. Methyl viologen dichloride hydrate ($C_{12}H_{14}Cl_2N_2$, 98%) was purchased from Sigma-Aldrich. Anhydrous sodium sulphate (Na_2SO_4, AR grade) was obtained from S.D. Fine-chem, India. Sodium 2-((4-aminophenyl) sulphonyl) ethyl hydrogen sulphate (APSEHS, commonly known as vinyl sulphone ester of aniline (VS)) and 1-amino-8 hydroxynaphthalene-3, 6-disulphonic acid (AHNDS, commonly known as H-Acid (HA)) were obtained from a local dye manufacturer. RB5 is manufactured by coupling two APSEHS molecules with one AHNDS molecule through two azo bonds.

2.2. Photocatalytic experiments

Photocatalytic experiments were performed in a cylindrical reactor fabricated from Plexiglas, as shown in Fig. 1. Five hundred millilitre aqueous solution of 50 mg L^{-1} RB5 dye was mixed with required doses of photocatalyst TiO_2 (P25) and HS, followed by pH adjustment and stirring for 30 min in dark to obtain adsorption-desorption equilibrium. The mixture was then irradiated by 11W UV light (Philips, UVC) with a light flux of 1.2 mW cm^{-2} (flux measured using pyranometer, Weather Technologies RN2104). To eliminate the electron-scavenging effect of dissolved oxygen, Argon gas was bubbled in the reactor during the entire experiment at 0.12 L min^{-1}. Contents of the reactor were mixed throughout the experiment by magnetic stirrer. 3 mL of suspension was sampled at regular time interval, centrifuged and the supernatant was analysed by UV-vis spectrophotometer. All the experiments were carried out at room temperature
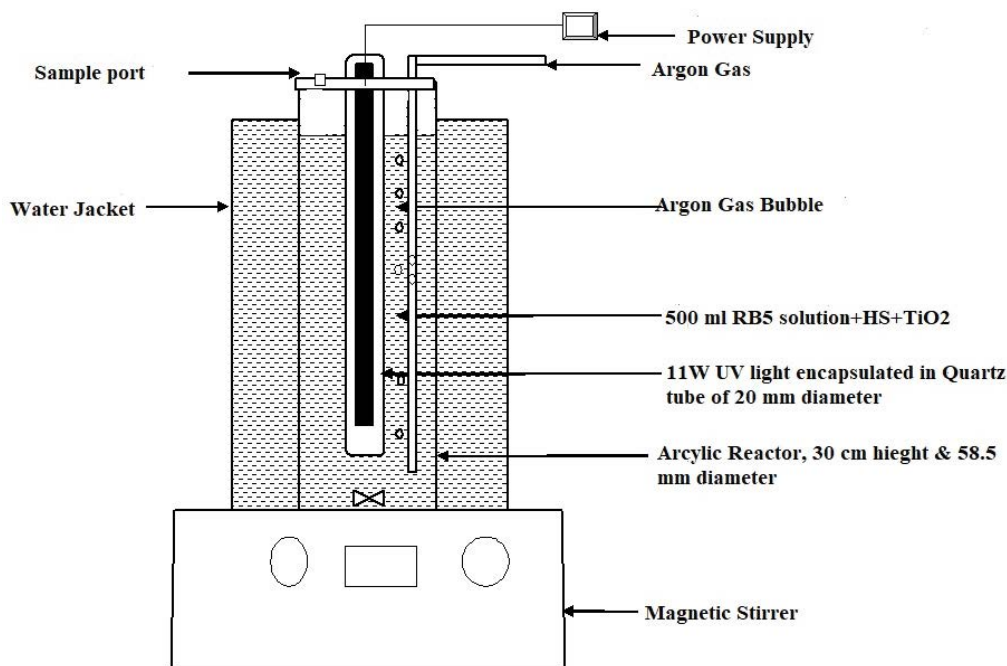
Fig. 1. Experimental setup for photocatalysis of RB5.

($33 \pm 2°C$). To control the temperature during the reaction, the reactor was placed in a water jacket having continuous circulation of water, which limited the rise in temperature to <1°C of the initial temperature during the irradiation period. All experiments were conducted in duplicate and average values of the results were reported.

2.2.1. Control experiments

In photocatalytic reactions, UV irradiation and TiO_2 particles may contribute significantly to removal of a target pollutant, individually or in combination, respectively by photolysis, and adsorption on TiO_2. Control experiments were carried out as: (1) RB5 solution + UV irradiation and (2) RB5 solution + HS + UV irradiation. The contribution of above combinations to RB5 decolourization was 6%–8% and 18%–30%, respectively. RB5 adsorption on TiO_2 particles, if any, in the absence of UV light (i.e., dark adsorption) was evaluated during each experiment. The reaction kinetics were evaluated considering RB5 concentration after dark adsorption as C_o (initial concentration), and beginning of UV irradiation as t_o (i.e., beginning of reaction).

2.3. Influence of various experimental parameters

The effect of various experimental parameters on the photocatalysis of RB5 was studied by varying the type of HS (OA, FA, methanol and IPA); concentration of HS (0.1 mM–4 mM); initial pH (2–9); initial RB5 concentration (50–200 mg L⁻¹) and dose of TiO_2 (0.125–2 g L⁻¹).

2.4. Reusability and regeneration of TiO₂

To check the reusability of TiO_2, the photocatalytic reaction was carried out for 20 min using fresh TiO_2. 20 min reaction period was chosen since RB5 decolourization by this time was ≥90%. Subsequent to this, residual RB5 concentration was measured, and RB5 stock solution was spiked into the reactor in such proportion that initial RB5 concentration for the second run becomes 50 mg L⁻¹. The procedure was repeated several times. TiO_2 particles reused for 5 cycles were subjected to FTIR analysis to determine the presence of functional groups due to adsorption of end products of RB5 decolourization. Used TiO_2 was regenerated by a simple procedure which involved: (1) washing several times with distilled water, (2) sonication of washed TiO_2 for 20 min in distilled water and (3) separation and drying.

2.5. Analytical methods

RB5 decolourization and generation of end-products were monitored using Agilent Cary 60 UV-vis single beam spectrophotometer by scanning the samples through 200–800 nm range. The percentage RB5 decolourization was calculated using Eq. (2) as follows:

$$\%Decolourization = \frac{(A_o - A)}{A_o} \times 100 \qquad (2)$$

where A_o = absorbance at 595 nm at time $t = 0$ of UV irradiation; A = absorbance at 595 nm at time $t = t$ of UV irradiation.

LC-MS analyses were performed in negative-ion mode on Nexera ultra high-performance liquid chromatography (UHPLC) system (Auto-sampler SIL 20 AC, Pump 20-ADvp, degasser DGU-20A5R, SHIMADZU) coupled with Ultra-Fast Triple Quardupole Liquid Chromatography and Mass Spectrometer (Nexera LCMS 8030, SHIMADZU). The interface potential was 4.5 kV. Nitrogen gas was used as nebulizer and drier gas at a flow rate of 3 and 15 L min⁻¹, respectively. Chromatographic separation was performed using Gemini C18 column (250 mm × 4.6 mm × 5 μm); oven

temperature: 40°C; two solvent mixtures were used (A: 95% H_2O, 5% acetonitrile, 25 mM ammonium acetate; B: 50% H_2O, 50% acetonitrile, 25 mM ammonium acetate) with the following conditions: 0–20 min 100% A; 20–25 min 50% A, 50% B; 25–30 min. 100% A; flow rate: 1 mL min^{-1}, pressure: 6.5 MPa, detection wavelength: 254 nm (Ref. [33]). The m/z range analyzed was from 10 to 1,000 m/z.

Light intensity in the photoreactor was determined using chemical actinometry by potassium ferrioxalate method outlined previously by Hatchard and Parker [34] and as described by Montalti et al. [35]. The light intensity was found to be 5.46 × 10^{-6} moles of photon/min. IR spectra of used TiO_2 were obtained using Nicolet 6700 FTIR.

3. Results and discussion

3.1. Screening of HS for PCR of RB5

Selection of a proper HS is very important since it plays a pivotal role in PCR. HS is sacrificially oxidized by the photogenerated holes, leaving the photogenerated electrons available for reduction and decreasing the recombination rate of electrons and holes.

Fig. 2 shows the time course profiles of RB5 decolourization in the presence of various HS. The initial concentration of each HS was 2 mM. The initial pH was set at 2.8. It may be noted from Fig. 2 that the initial rate as well as the extent of RB5 removal after 60 min of irradiation were significantly lesser in the presence of methanol and IPA than that of OA and FA. Dark adsorption was found to be around 2%, 23%, 17% and 17%, respectively, in the presence of OA, FA, Methanol and IPA, as HS. Although, the dark adsorption was significantly higher in the presence of FA, once the irradiation started, the rate of RB5 decolourization was more rapid in the presence of OA. It may be noted that the pKa of FA (HCOOH) is 3.75 and point of zero charge (pzc) of TiO_2 is well reported in literature as 6.25. Thus, at pH 2.8, more than 80% FA will exist as HCOOH while TiO_2 will be positively charged. On the other hand, the sulphonic groups of RB5 will exist as SO_3^- at this pH. Thus, negatively charged RB5 will be adsorbed on positively charged TiO_2 at pH 2.8 without much interference from FA in form of HCOOH. On the other hand, pKa_1 of OA is 1.27, and at pH 2.8, most of it will exist as $HC_2O_4^-$ ions which may compete with negatively charged RB5 for adsorption, resulting in lesser RB5 adsorption on TiO_2.

It is reported that reaction of FA and OA with photogenerated holes leads to formation of strongly nucleophilic carboxyl anion radical $CO_2^{\bullet-}$ ($E^0 \left(CO_2 / CO_2^{\bullet-} \right)$ = –1.85 V [18,20]) as shown in Eq. (3) [24–25] and Eq. (4) [18–19]. This may be the cause of superior rate and extent of RB5 decolourization obtained in the presence of OA and FA.

$$HCOO^- + h^+ \rightarrow H^+ + CO_2^{\bullet-} \tag{3}$$

$$C_2O_4^{2-} + h^+ \rightarrow CO_2 + CO_2^{\bullet-} \tag{4}$$

In addition to the formation of $CO_2^{\bullet-}$, in oxygen-free atmosphere, oxalate ion may be oxidized by photogenerated holes resulting in the formation of oxalate radical
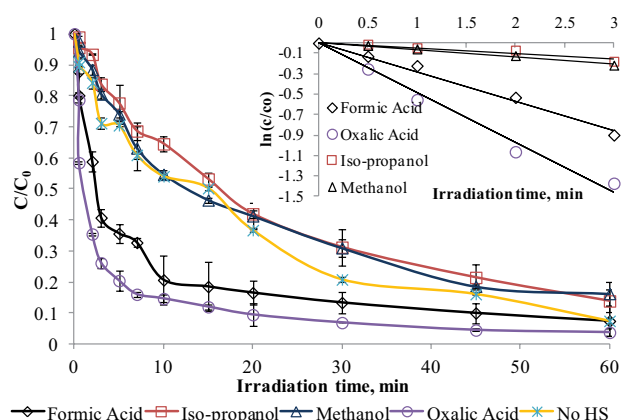

Fig. 2. Time course profile of RB5 decolourization using different hole scavengers. (*Reaction conditions*: Reaction volume, 500 mL; Initial RB5 concentration, 50 mg L^{-1}; HS concentration, 2 mM; TiO_2 concentration, 0.5 g L^{-1}; Initial pH 2.8; C_0 represents RB5 concentration after dark adsorption.)

$C_2O_4^{\bullet-}$ [$\left(E^0 \left(C_2O_4^{2-} / C_2O_4^{\bullet-} \right) = -2.1 \text{ V} [19] \right)$ as shown in Eq. (5) as follows:

$$C_2O_4^{2-} + h^+ \rightarrow C_2O_4^{\bullet-} \tag{5}$$

Oxalate radical thus formed having strong reduction potential, may also be responsible for OA demonstrating superior RB5 decolourization rate as compared with other HS attempted in this study.

Figs. 3(a)–(d) show UV-vis spectra of reaction solution at various time points in the presence of methanol, IPA, FA and OA, respectively. As revealed in Fig. 3, at t = 0, three distinct peaks viz., 254, 312 and 595 nm could be seen. It is interesting to note that the UV-vis spectra in case of FA (Fig. 3(c)) and OA (Fig. 3(d)) show significant increase in absorbance at 254 nm with concomitant decrease in peak at 595 nm; however, such an increase, if any, in case of methanol (Fig. 3(a)) and IPA (Fig. 3(b)) is negligible. Increase in the absorbance at 254 nm (for FA and OA) may be attributed to formation and accumulation of intermediates/end-products. Patel et al. [32] studied RB5 decolourization using electrocoagulation employing iron sacrificial anode. The authors noted increase in absorbance at 265 nm concomitant with RB5 decolourization and attributed it to the formation of VS by cleavage of azo bonds. Popli and Patel [36] demonstrated electrocatalytic reduction of RB5 and noted increase in absorbance at 254 nm. The authors identified the compound at 254 nm as sodium 2-[(4-aminopheynyl) sulphonyl] ethyl sulphate (ABSES) formed due to cleavage of azo (N=N) bonds.

Since increase in the absorbance at 254 nm is correlated with the reductive cleavage of the azo bonds and concomitant release of aromatic amines, the insignificant increase in the absorbance at 254 nm may suggest that the probable pathway for RB5 decolourization may not be complete cleavage of azo bonds in the presence of methanol and IPA as HS. Thus, methanol and IPA appear to be the HSs inferior to OA and FA. Thus, further investigation on PCR of RB5 decolourization was carried out using OA as an HS.
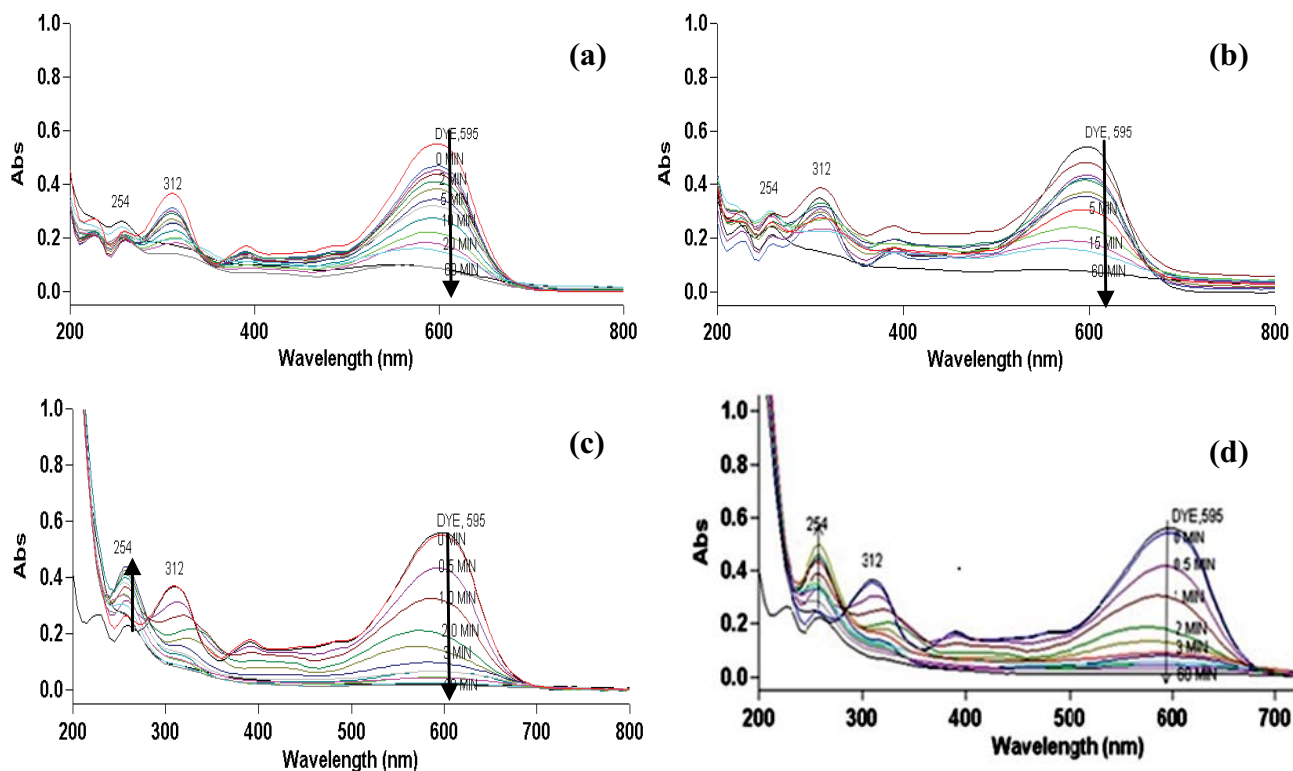
Fig. 3. UV-vis spectra showing RB5 decolourization using: (a) methanol, (b) IPA, (c) FA, and (d) OA as HS. (*Reaction conditions:* Reaction volume, 500 mL; Initial RB5 concentration, 50 mg L^{-1}; HS concentration, 2 mM; TiO$_2$ concentration, 0.5 g L^{-1}; Initial pH.2.8.)

3.2. PCR of RB5 using oxalic acid as a HS

Fig. 4 shows time course profile of RB5 decolourization obtained using 0.5 g L^{-1} TiO$_2$ and 2 mM OA at initial pH 2.8 (pH of RB5 solution containing 2 mM OA). As seen from Fig. 4, RB5 decolourization was very rapid with >80% decolourization achieved in the first 5 min of irradiation. The extent of RB5 decolourization at the end of 1 h of irradiation was around 96%. It may also be noted that the dark

adsorption of RB5 on the surface of TiO$_2$ was insignificant (ca. 2%) for the given experimental conditions. The inset in Fig. 4 shows that photocatalytic decolourization of RB5 fitted well into pseudo-first-order reaction model. In the first-order reaction plot, time t = 0 min and initial RB5 concentration (C_o) represent the beginning of irradiation and the RB5 concentration at the end of dark adsorption, respectively.

LC-MS analysis was performed on a sample withdrawn following 3.0 min of irradiation. Fig. 5(a) shows HPLC chromatogram represented by a sharp peak at RT of 8.1 min and a group of peaks between RT 2.5 and 3.5 min. The group of peaks may represent the intermediate and its degraded parts. The degradation of intermediate may be attributed to photolysis or photocatalytic reactions. The HPLC chromatogram of aqueous solution of 2-((4-aminophenyl) sulphonyl) ethyl hydrogen sulphate (APSEHS) detected the compound at RT ~8 min (APSEHS chromatogram is not shown here). Fig. 5(b) shows mass spectrum of intermediate detected at RT of 8.1 min. The mass spectrum shows two main m/z peaks; one at 280 representing ionized form of APSEHS (M-H, molecular weight 280 g mol^{-1}) and another at 170.9 representing fragmented form of APSEHS (M-CH$_2$-OSO$_3$, molecular weight 171 g mol^{-1}). Thus, the compound detected at RT 8.1 min was identified as APSEHS. Fig. 5(c) shows mass spectrum of compound at RT 2.7 min represented by three main m/z peaks: 299, 221 and 179. Considering probable chemical structures shown in Fig. 5(c) and chemical structure of RB5, it seems that the compound detected at RT 2.7 min must be a degraded form of 3,4,6-triamino-5-hydroxynaphthalene-2,7-disulphonic acid (TAHNDS). Based on these results, it was concluded
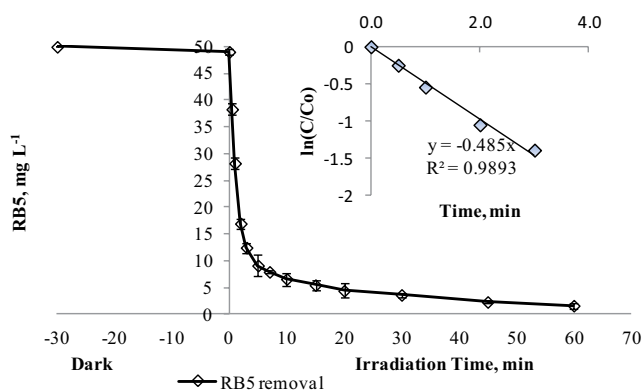

Fig. 4. Time course profile of RB5 decolourization (–30 to 0 min shows time for dark adsorption) in the presence of OA as HS. Inset shows corresponding first-order kinetics plot. (*Reaction conditions:* Reaction volume, 500 mL; Initial RB5 concentration, 50 mg L^{-1}; OA concentration, 2 mM; TiO$_2$ concentration, 0.5 g L^{-1}; Initial pH 2.8.)
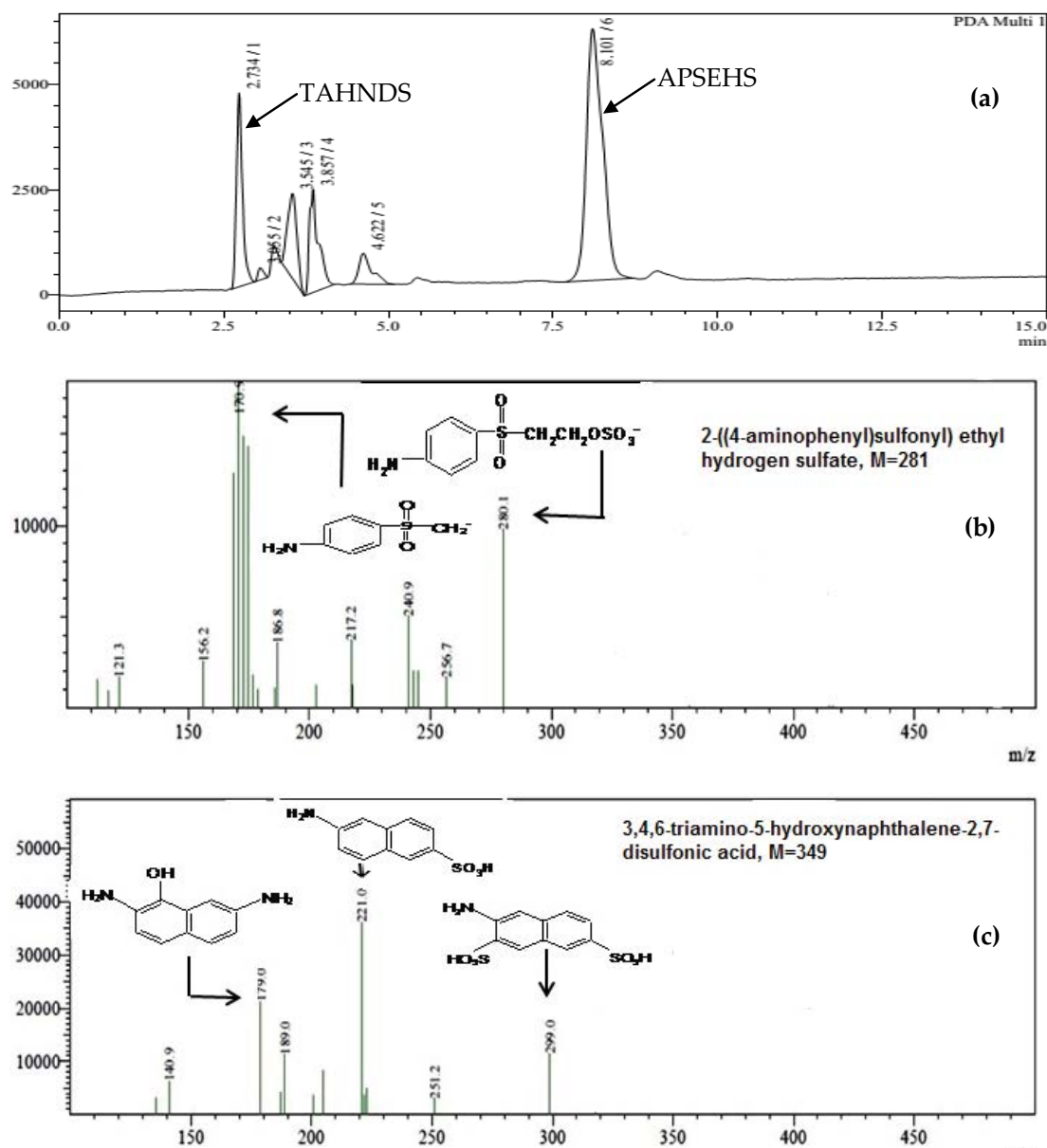
Fig. 5. (a) HPLC Chromatograms obtained at 254 nm, (b) Mass spectrum of compound having RT of 8.1 min, (c) Mass spectrum of compound having RT of 2.7 min. (*Reaction conditions:* Reaction volume, 500 mL; Initial RB5 concentration, 50 mg L^{-1}; OA concentration, 2 mM; TiO$_2$ concentration,0.5 g L^{-1}; Initial pH 2.8.)

that reductive decolourization of RB5 proceeds via cleavage of azo bonds as shown in Fig. 6 [2,32,33]. Intermediates identical to the ones detected in the study have been identified and cleavage of azo bonds as decolourization mechanism has been proposed by other authors studying reductive decolourization of RB5. For instance, Libra et al. [33] detected 1,2-ketimino-7-amino-8-hydroxynaphthalene-3,6 disulphonic acid and *p*-aminobenzene-2-hydroxyl ethyl sulphonic acid (*p*-ABHES) as intermediates during anaerobic reduction of RB5. Patel and Suresh [37] detected 1-sulphonic, 2-(4-amino-benzenesulphonyl) ethanol and 1-2-7-triamino-8-hydroxy, 3-6-naphthaline disulphonate as intermediates using Mg-Pd bimetallic system for reduction of RB5.

Based on earlier discussion, and end-products detected by LC-MS; a mechanism of reductive RB5 decolourization in the presence of OA as HS is shown in Fig. 7.

3.3. Effect of TiO$_2$ dose on RB5 decolourization

The effect of photocatalyst concentration on PCR of RB5 was studied by varying the concentration of TiO$_2$ from 0.125 to 2 g L^{-1}, keeping other parameters constant. %RB5 decolourization at all the concentrations of TiO$_2$ was found to be nearly the same (ca. 96%) at the end of 60 min of irradiation. However, as seen from Table 1, the first-order reaction rate constant increased significantly with increase in
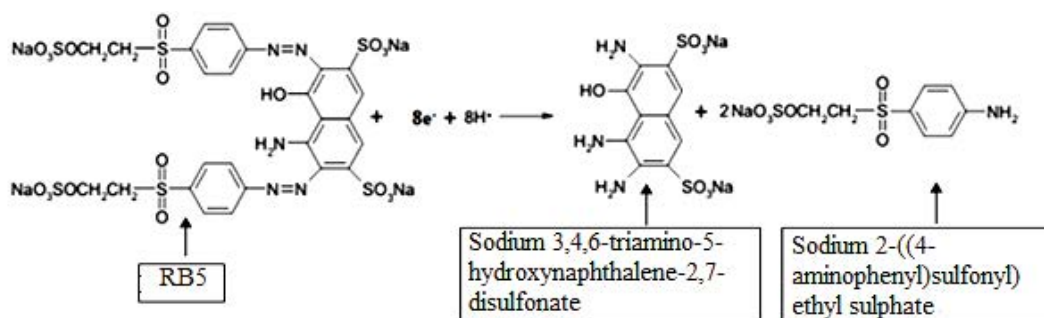
Fig. 6. Photocatalytic reduction of RB5 and formation of aromatic intermediates due to cleavage of azo bonds.
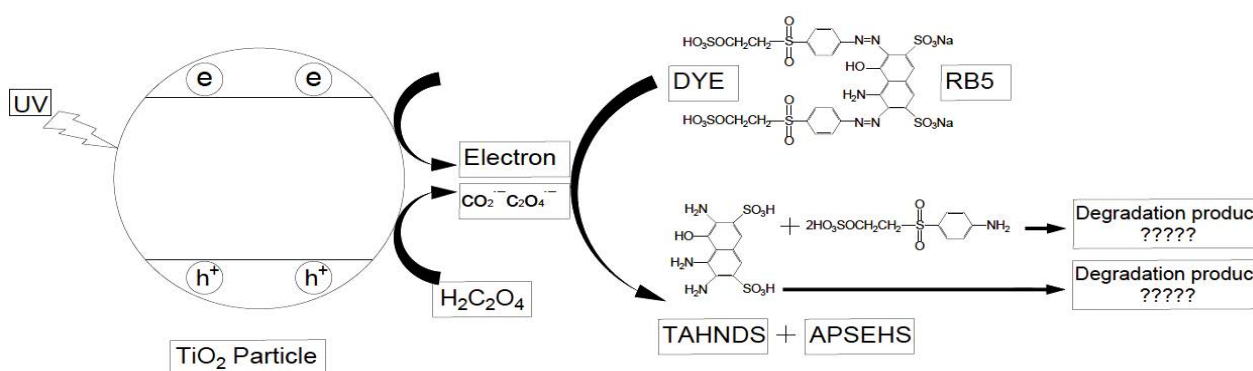

Fig. 7. Mechanism of photocatalytic reduction of RB5 in the presence of oxalic acid as a hole scavenger.

Table 1
First-order RB5 decolourization rate constants at various doses of TiO_2

Concentration of TiO_2 (g L^{-1})	First-order reaction rate constant (min^{-1})
0.125	0.34
0.25	0.39
0.5	0.48
1	0.53
1.5	0.53
2	0.51

concentration of TiO_2 up to 1 g L^{-1}, beyond which, the rate constant remained unchanged.

The increase in the rate of reaction with increase in TiO_2 dose may be attributed to increase in number of active sites. However, further increase in TiO_2 dose might have the following adverse effects: (1) scattering and screening of UV radiation and (2) agglomeration of TiO_2 particles leading to reduction in surface area available for absorption of UV radiation [12,38–39]. Since there was no significant change in the first-order reaction rate constant at higher concentrations, 1 g L^{-1} TiO_2 was selected for further study. Optimum dose of TiO_2 as 1 g L^{-1} has been reported in PCR studies on various pollutants like nitrate [11], copper [23] and selenium [23]. On the other hand, optimum TiO_2 concentrations ranging between 0.3 and 8.0 g L^{-1} have been reported for PCO of pesticides and phenolic compounds [38].

3.4. Effect of dose of OA on RB5 decolourization

Concentration of HS plays an important role in achieving PCR of a pollutant. A small concentration of HS cannot scavenge all the holes and make available sufficient electrons for reduction. In such a situation PCO may also contribute significantly to destruction of dye. The effect of varying dose of OA (0.1–4 mM) on RB5 decolourization was studied at initial pH 2.8–2.9. Table 2 shows effect of OA dose on first-order decolourization rate constant and maximum absorbance at 254 nm ($A_{254\ (max)}$) reached during these experiments. At all the OA concentrations attempted, the RB5 decolourization at the end of 60 min irradiation was ≥90%.

As seen from Table 2, the first-order reaction rate constant increases with increase in OA concentration from 0.1 to 0.5 mM. Such an observation can be attributed to the availability of more valance bond electrons for reduction of RB5 as more numbers of holes will be neutralized by sacrificial oxidation of OA. Also the concentration of reducing radicals such as $CO_2^{•-}$ and $C_2O_4^{•-}$ will increase, thereby causing rapid decolourization of RB5 over and above that by electrons. With further increase in OA concentration from 0.5 to 2 mM, the first-order reaction constant increases gradually and plateaus at 2 mM. As explained earlier, at pH 2.8, OA will predominantly exist as $HC_2O_4^-$. With increase in OA, $HC_2O_4^-$ concentration will also increase. Since RB5 is also negatively charged at this pH, increased concentration of $HC_2O_4^-$ may interfere with the contact of RB5 with active sites on TiO_2 surface. In such a situation, reduction of azo bonds may be

Table 2
Effect of concentration of OA on the rate of PCR of RB5 and by-product generation

HS dose (mM)	First-order reaction rate constant (min^{-1})	Maximum absorbance at 254 nm($A_{254(max)}$)	Time to reach $A_{254(max)}$
0.1	0.3665	0.5564	5
0.25	0.43725	0.6578	5
0.5	0.504	0.6940	3
1	0.509	1.0388	3
1.5	0.526	1.0615	3
2	0.537	1.0641	3
4	0.537	1.0455	3

restricted since reduction by photogenerated electrons is a surface phenomenon.

Moreover, as seen from Table 2, the maximum absorbance at 254 nm ($A_{254 (max)}$) increased with increase in OA dose indicating greater PCR at higher OA doses. Thus, it seems that OA concentrations ≤0.25 mM may not be sufficient to scavenge all the holes and sustain PCR of RB5. Considering the results depicted in Table 2, OA dose of 2 mM was employed for further experiments.

3.5. Contribution of reductive species to RB5 decolourization

The proposed mechanism of RB5 decolourization involves reduction by photogenerated electrons and reducing radicals such as carboxyl ($CO_2^{\bullet-}$) and oxalate ($C_2O_4^{\bullet-}$). Electron scavenger (sulphate ions, 1.75 mM) and carboxyl radical scavenger (methyl viologen (MV), 0.1 mM) were used to evaluate the contribution of each of them in reductive decolourization of RB5. The use of MV as scavenger of carboxyl radical has been demonstrated by Gu et al. [40] and Berkovic et al. [41]. On the other hand, sulphate ions get oxidized by holes of valance band or hydroxyl radicals to persulphate ions. Persulphate ions thus formed act as electron acceptors as presented in Eq. (6) as follows [42]:

$$S_2O_8^{-2} + e_{cb}^- \rightarrow SO_4^- + SO_4^{2-} \tag{6}$$

Fig. 8 shows the effect of these scavengers on the kinetics of RB5 decolourization. The first-order reaction rate constants obtained with and without the use of scavengers were used to determine the role of electron, carboxyl radical and oxalate radicals on RB5 decolourization. The first-order reaction rate constant k_{RB5} in the absence of any scavengers can be shown as in Eq. (7) as follows:

$$k_{RB5} = k_e + k_{CO_2^{\bullet-}} + k_{C_2O_4^{\bullet-}} \tag{7}$$

where k_e, $k_{CO_2^{\bullet-}}$ and $k_{C_2O_4^{\bullet-}}$, respectively, represent decolourization due to electrons, $CO_2^{\bullet-}$ and $C_2O_4^{\bullet-}$.

Let k_1 be the reaction rate constant in the presence of sulphate ions as electron scavenger. Thus,

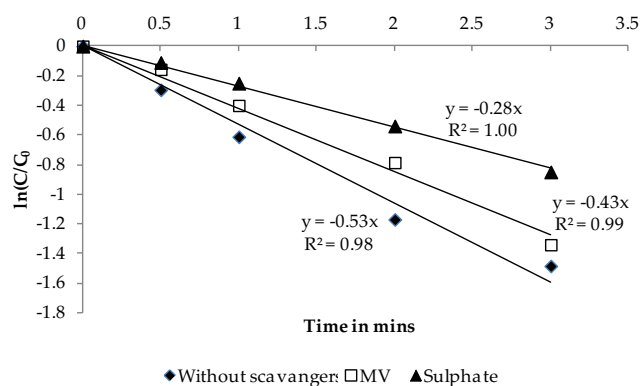$$k_1 = k_{CO_2^{\bullet-}} + k_{C_2O_4^{\bullet-}} \tag{8}$$

Fig. 8. First order kinetic plots of RB5 decolourization in the presence of various scavengers of reductive species. (*Reaction conditions:* Reaction volume, 500 mL; Initial RB5 concentration, 50 mg L^{-1}; HS concentration, 2 mM; TiO$_2$ concentration, 1 g L^{-1}; Initial pH.2.8.)

Let k_2 be the reaction rate constant in the presence of methyl viologen as carboxyl radical scavenger. Thus,

$$k_2 = k_e + k_{C_2O_4^{\bullet-}} \tag{9}$$

From Eqs. (7), (8) and (9) as follows:

$$k_{RB5} = k_1 + k_2 - k_{C_2O_4^{\bullet-}} \tag{10}$$

Substituting the values of respective first-order reaction rate constants (see Fig. 8) in Eq. (10), we get

$$0.53 = 0.28 + 0.43 - k_{C_2O_4^{\bullet-}}$$

$$\therefore k_{C_2O_4^{\bullet-}} = 0.18 \, min^{-1}.$$

Substituting value of $k_{C_2O_4^{\bullet-}}$, k_e and $k_{CO_2^{\bullet-}}$ were found to be 0.25 and 0.1 min^{-1}, respectively. This shows that contribution of electron in reductive decolourization of RB5 was about 47%, while that of $CO_2^{\bullet-}$ radical was 19% and $C_2O_4^{\bullet-}$ was 34%. Thus, photogenerated electrons (e_{cb}^-) and oxalate radicals contributed mainly (>80%) to RB5 decolourization.

3.6. Effect of initial pH on photocatalytic decolourization of RB5

The effect of varying initial pH (2–9) on RB5 decolourization was studied at a constant OA dose of 2 mM. The extent of RB5 decolourization at the end of 60 min of irradiation was found to range from 94% to 95%, at all the initial pH values except 2.0, 7.0 and 9.0, where decolourization was ~ 88%–89%. As seen from Table 3, the first-order RB5 decolourization rate constant decreased with increase in initial pH and the highest first-order reaction constant ($k = 0.535$ min^{-1}) was obtained at initial pH 2.8.

The pzc of TiO$_2$ (Evonik/Degussa P25) is widely investigated/reported at pH~6.25 [38–39]. As shown in Eqs. (11) and (12), under acidic conditions (pH < 6.25), the TiO$_2$ surface

Table 3
First-order RB5 decolourization rate constant at varying initial pH values

Initial pH of dye solution	First-order reaction rate constant (min^{-1})
2	0.205
2.8	0.535
3.5	0.38
4	0.38
4.5	0.35
5	0.24
6	0.14
7	0.03
9	0.038

Reaction conditions: RB5, 50 mg L^{-1}; TiO_2, 1 g L^{-1}; HS, 2 mM OA.

will be positively charged, while under alkaline conditions (pH > 6.25), negatively charged.

$$pH < P_{zc} \quad TiOH + H^+ \rightarrow TiOH_2^+ \tag{11}$$

$$pH > P_{zc} \quad TiOH + OH^- \rightarrow TiO^- + H_2O \tag{12}$$
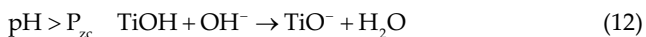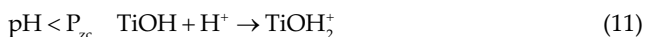
Since RB5 is an electronegative dye (due to HSO_3^-), it will have higher affinity toward positively charged TiO_2 at acidic pH leading to better mass transfer and decolourization. Moreover, it has been suggested that the photogenerated electron reach more readily to the catalyst surface when TiO_2 is positively charged. [21,43]. On the other hand, at pH > 6.25, TiO_2, RB5, and $HC_2O_4^{-1}$ and $C_2O_4^{-2}$ from OA; all will be negatively charged, reducing the affinity of HS and the target compound for TiO_2, resulting into slower and partial PCR. Tan et al. [22] reported the highest reduction of selenium ions using TiO_2 in the acidic pH range of 2.2–4, with the highest removal being obtained at initial pH 2.2. Thus, initial pH greatly influenced the rate and extent of RB5 decolourization.

Fig. 9 shows the maximum absorbance at 254 nm ($A_{254 (max)}$) and the time ($t_{254 (max)}$) to reach the same at different initial pH values. Although, RB5 decolourization at pH ranging from 2.8 to 6 was 94%–95% (i.e., identical); the $A_{254 (max)}$ decreased with increase in pH from 2.8 to 6.0. Since the increase in absorbance at 254 nm is result of PCR of RB5, decrease in $A_{254 (max)}$ with increase in pH (pH range 2–6) suggests that PCO may also contribute to RB5 decolourization in this pH range. With increase in pH, concentration of OH^- and therefore $OH\bullet$ increases; resulting in increased consumption of HS and decreased chances of PCR. Consistent with foregoing discussion, it may be observed that $t_{254(max)}$ increases gradually from 3 to 10 min with increase in initial pH from 2.8 to 6.0 followed by sudden increase in $t_{254(max)}$ to 45 min at pH 7 and 9. This is attributed to slower generation and accumulation of aromatic amines due to slower PCR of RB5 with increase in initial pH.

Based on the results obtained from experiments exploring influence of various parameters, following set of optimum
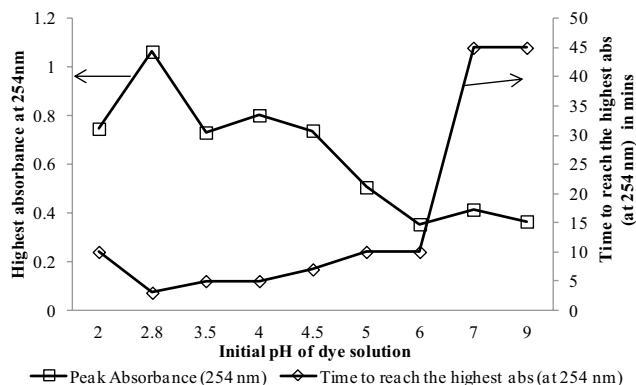

Fig. 9. Highest absorbance at 254 nm and time to reach the same with respect to varying initial pH values. (*Reaction conditions:* RB5, 50 mg L^{-1}; TiO_2, 1 g L^{-1}; HS, 2 mM OA.)

parameters was obtained: HS concentration, 2 mM OA; TiO_2 concentration, 1 g L^{-1} and initial pH~2.8. Fig. 10 shows the % decolourization of RB5 obtained using optimized parameters.

Table 4 shows the comparison of results obtained in the present study with the published reports demonstrating reductive decolourization of RB5.

3.7. Effect of initial dye concentration

The usual concentration of dyes in textile industry effluents ranges between 50 and 250 mg L^{-1} [14]. Fig. 11 shows effect of initial RB5 concentration on decolourization. The decolourization after 60 min of irradiation was found be more or less same (ca. 94%). But the first-order reaction rate constant decreased with increase in the initial concentration of RB5 (see inset of Fig. 11). This can be explained by the fact that according to the Beer–Lambert law, with increase in initial dye concentration, the fraction of photons reaching the photocatalyst decreases [14,44]. However, with irradiation, as dye concentration in the solution decreases, the number of photon reaching photocatalyst increases resulting in almost similar extent of decolourization after 60 min for all the dye concentrations tried. A distinct peak at 254 nm was found in
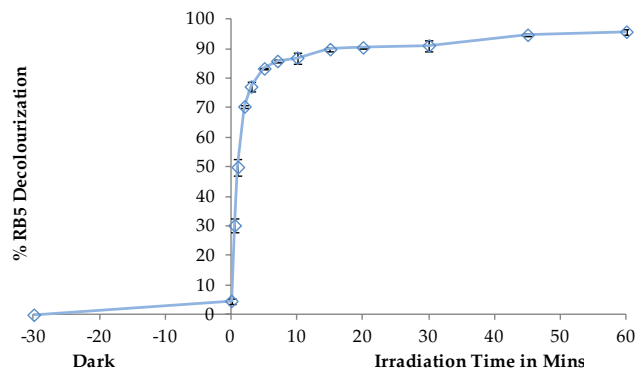

Fig. 10. PCR of RB5 at optimum experimental parameters. (*Reaction conditions:* Reaction volume, 500 mL; Initial RB5 concentration, 50 mg L^{-1}, HS concentration, 2 mM OA; TiO_2 concentration, 1 g L^{-1}; Initial pH~2.8.)

Table 4
Comparison of results obtained from the present study with the published literature

| Authors	Method of treatment	Experimental conditions	Results	
			% decolourization	First order reaction rate constant (min^{-1})
Present study	Photocatalytic reduction	RB5 concentration: 50 mg L^{-1}, OA dose: 2 mM, TiO$_2$ dose:1g L^{-1} and pH:2.8	95.75% in 60 min	0.53
[33]	Two stage anaerobic/aerobic bacterial process	RB5 concentration: 1.25 g L^{-1}	65% in 15 h	Not reported
[37]	Magnesium-palladium bimetallic system	RB5 concentration: 100 mg L^{-1} and 17.5 mg L^{-1} Pd^{+4} as catalyst	80% in 60 min	0.51
[32]	Electrocoagulation using iron sacrificial anode	RB5 concentration: 100 mg L^{-1} and 7.5 mA cm^{-2} current density	90% in 60 min	0.13
[36]	Electro-catalytic reduction	RB5 concentration: 50 mg L^{-1}, 10 mM AgNPs, and 10 mA cm^{-2} current density	99% in 180 min	0.043
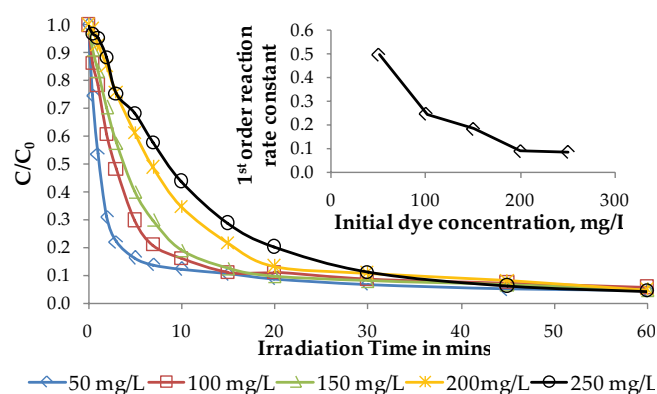
Fig. 11. Time course profiles of RB5 decolourization at varying initial RB5 concentrations. Inset shows corresponding first-order reaction rate constant. (*Reaction conditions:* Reaction volume, 500 mL; HS concentration, 2 mM OA; TiO$_2$ concentration, 1 g L^{-1}; Initial pH~2.8.)

UV-vis spectra obtained for all the dye concentrations tried, indicating that PCR of RB5 was possible even at a very high concentration of 250 mg L^{-1}. The rate as well as the quantity of amines generated though decreased with increase in initial concentration of dye. This can be due to the fact that; since HS dose was kept constant, the number of electrons as well as the reducing radicals available remained the same, resulting in lower rate of decolourization and lesser quantity of amines generated during PCR.

3.8. Reusability of TiO$_2$

The %RB5 decolourization at the end of 20 min reaction period gradually decreased from ~92% at the first use to 64% at the fifth reuse. This shows that TiO$_2$ maintains significant photocatalytic activity even at the fifth reuse. The UV-vis spectra of RB5 solution after each reuse showed increase in absorbance at 254 nm, indicating that TiO$_2$ performed PCR even after five reuses though at a decreasing rate. To investigate the reason behind reduction in catalytic activity used

TiO$_2$ particles were analysed by FTIR. FTIR analysis revealed the presence of peaks corresponding to ester (related to APSEHS, wave-number 1,718 cm^{-1}), aromatic ring (asymmetric stretch, wave-number 1,400 cm^{-1}), and C-N amines (wave-number 1,230 cm^{-1}) indicating that adsorption of end products of RB5 may be responsible to decrease photocatalytic activity. TiO$_2$ particles following five reuses were regenerated. The decolourization efficiency obtained using regenerated TiO$_2$ was less by only 2% (i.e., ca. 90%) as compared with the fresh TiO$_2$ particle. However, the rate of RB5 decolourization using regenerated TiO$_2$ was significantly less than that using fresh TiO$_2$. This may be attributed to reduced surface area of TiO$_2$ probably due to agglomeration during centrifugation and drying.

4. Conclusion

- TiO$_2$ exhibited excellent reductive photocatalytic activity in the presence of OA and FA as HS by decolourizing more than 94% of initial 50 mg L^{-1} RB5 at initial pH of 2.8 in less than 1h reaction time.
- Among methanol, IPA, FA and OA, used as HS; OA yielded the maximum extent and rate of RB5 decolourization, due to its capacity to produce strong reductive radicals; $CO_2^{\bullet-}$ and $C_2O_4^{\bullet-}$, in addition to scavenge the photogenerated holes. The first-order RB5 decolourization rate constant increased with increase in concentration of TiO$_2$ and OA up to certain concentrations and then remained constant with further increase in concentrations. LC-MS analysis revealed APSEHS and TAHNDS as end-products of RB5 decolourization suggesting that PCR of RB5 proceeded through cleavage of azo bonds.
- Type and concentration of HS greatly influenced the rate of RB5 decolourization and the rate well as the concentration of amines (end products) produced.
- Photogenerated electrons (e_{cb}^-), oxalate radicals and carboxyl radicals contributed to RB5 decolourization respectively by 47%, 34% and 19%. Thus, e_{cb}^- and $C_2O_4^{\bullet-}$ radicals were main reductive species responsible for RB5 decolourization.

- The initial pH value greatly influenced not only the rate of PCR of RB5 but also the rate of amines (end products) generation and time to achieve the peak concentration of amines accumulated in the reactor. In the pH range of 2.0–9.0, the highest rate and extent of RB5 decolourization were achieved at initial pH 2.8.
- TiO_2 exhibited good reusability. More than 90% RB5 decolourization at the first use decreased to 64% at the fifth use. Adsorption of end-products of RB5 decolourization and/or their degraded products seems responsible for the decrease in photocatalytic activity of TiO_2. The regenerated TiO_2 could achieve ca. 90% RB5 decolourization; however, the rate of reaction was significantly lower than that of fresh TiO_2.

References

[1] Z. Xu, M. Zhang, J. Wu, J. Liang, L. Zhou, B. Lu, Visible light-degradation of azo dye methyl orange using TiO_2/β-FeOOH as a heterogeneous photo-Fenton-like catalyst. Water Sci. Technol., 68 (2013) 2178–2185.

[2] S. Popli, U.D. Patel, Destruction of azo dyes by anaerobic–aerobic sequential biological treatment: a review, Int. J. Environ. Sci. Technol., 12 (2015) 405–420.

[3] H. Zhang, H. Gao, C. Cai, C. Zhang, L. Chen, Decolorization of crystal violet by ultrasound/heterogeneous Fenton process. Water Sci. Technol., 68 (2013) 2515–2520.

[4] H. Lan, A. Wang, R. Liua, H. Liua, J. Qua, Heterogeneous photo-Fenton degradation of acid red B over Fe_2O_3 supported on activated carbon fiber. J. Hazard. Mater., 285 (2015) 167–172.

[5] B. Cuiping, X. Xianfeng, G. Wenqi, F. Dexin, X. Mo, G. Zhongxue, X. Nian, Removal of Rhodamine B by ozone-based advanced oxidation process, Desalination, 278 (2011) 84–90.

[6] W. Chou, C. Wang, C. Chang, Comparison of removal of Acid Orange 7 by electrooxidation using various anode materials, Desalination, 266 (2011) 201–207.

[7] A.L. Linsebigler, G. Lu, J.T. Yates, Photocatalysis on TiO_2 surfaces; principles, mechanisms, and selected results, Chem. Rev., 95 (1995) 735–758.

[8] M. Maruganandham, M. Swaminathan, Solar photocatalytic degradation of a reactive dye in TiO_2- suspension, Sol. Energy Mater. Sol. Cells, 81 (2004) 439–457.

[9] L. Yin, J. Niu, Z. Shen, J. Chen, Mechanism of reductive decomposition of pentachlorophenol by Ti-Doped β-Bi_2O_3 under visible light irradiation, Environ. Sci. Technol., 44 (2010) 5581–5586.

[10] M.R. Hoffman, S.T. Martin, W.Y. Choi, D.W. Bahnemannt, Environmental applications of semiconductor photocatalysis, Chem. Rev., 95 (1995) 69–96.

[11] K. Doudrick, O. Monzon, A. Mangonon, K. Hristovski, P. Westerhoff, Nitrate reduction in water using commercial titanium dioxide photocatalysts (P25, P90 and Hombikat UV 100), J. Environ. Eng., 138 (2012) 852–861.

[12] L.B. Reutergardh, M. Iangphasuk, Photocatalytic decolourization of reactive azo dye: a comparison between TiO_2 and CdS photocatalysis, Chemosphere, 35 (1997) 585–596.

[13] M. Chong, Y. Cho, P. Poh, B. Jin, Evaluation of titanium dioxide photocatalysis technology for the treatment of reactive Black 5 dye in synthetic and real grey water effluents, J. Clean. Prod., 89 (2015) 196–202.

[14] K. Soutsas, V. Karayannis, I. Poulios, A. Riga, K. Ntampegliotis, X. Spiliotis, G. Papapolymerou, Decolourization and degradation of reactive azo dyes via heterogeneous photocatalytic processes, Desalination, 250 (2010) 345–350.

[15] X. Zhou, H. Ji, X. Haung, Photocatalytic degradation of methyl orange over metalloporphyrins supported on TiO_2 Degussa P25, Molecules, 17 (2012) 1149–1158.

[16] C. Hung, P. Chiang, C. Chou, Photocatalytic degradation of azo dye in TiO_2 suspended solution, Water Sci. Technol., 43 (2001) 313–320.

[17] D. Pathania, D. Gupta, A. Al-Muhtaseb, G. Sharma, A. Kumar Mu. Naushad, T. Ahamad, S. Alshehri, Photocatalytic degradation of highly toxic dyes using chitosan-g-poly(acrylamide)/ZnS in presence of solar irradiation, J. Photochem. Photobiol. A, 329 (2016) 61–68.

[18] R. Jin, W. Gao, J. Chen, H. Zeng, F. Zhang, Z. Liu, N. Guan, Photocatalytic reduction of nitrate ion in drinking water by using metal loaded $MgTiO_3$-TiO_2 composite semiconductor catalyst, J. Photochem. Photobiol. A. Chem., 162 (2004) 585–590.

[19] Y. Wang, P. Zhang, Photocatalytic decomposition of per-fluorooctanoic (PFOA) by TiO_2 in the presence of oxalic acid, J. Hazard. Mater., 192 (2011) 1869–1875.

[20] Y. Li, F. Wasgestian, Photocatalytic reduction of nitrate ions on TiO_2 by oxalic acid, J. Photochem. Photobiol. A. Chem., 112 (1998) 255–259.

[21] K. Doudrick, T. Yang, K. Hristovski, P. Westerhoff, Photocatalytic nitrate reduction in water: managing the hole scavenger and reaction by-product selectivity, Appl. Catal. B, 136–137 (2013) 40–47.

[22] T. Tan, D. Beydoun, R. Amal, Effects of organic hole scavengers on the photocatalytic reduction of selenium anions, J. Photochem. Photobiol. A., 159 (2003) 273–280.

[23] N. Aman, T. Mishra, J. Hait, R.K. Jana, Simultaneous photo-reductive removal of copper (II) and selenium (IV) under visible light over spherical binary oxide photocatalyst, J. Hazard. Mater., 186 (2011) 360–366.

[24] F.X. Zhang, R.C. Jin, J.X. Chen, C.Z. Shao, W.L. Gao, L.D. Ni, N.J. Guan, High photocatalytic activity and selectivity for nitrogen in nitrate reduction on Ag/TiO_2 catalyst with fine silver clusters, J. Catal., 232 (2005) 424–431.

[25] V.N.H. Nguyen, R. Amal, D. Beydoun, Effect of formate and methanol on photoreduction/removal of toxic cadmium ions using TiO2 semiconductor as photocatalyst, Chem. Eng. Sci., 58 (2003) 4429–4439.

[26] N. Serpone, I. Texier, A.V. Emeline, P. Pichat, H. Hidaka, J. Zhao, Post-irradiation effect and reductive dechlorination of chlorophenols at oxygen-free TiO_2/water interfaces in the presence of prominent hole scavengers, J. Photochem. Photobiol. A., 136 (2000) 145–155.

[27] K. Kabra, R. Chaudhary, R.L. Sawhney, Solar photocatalytic removal of Cu(II), Ni(II), Zn(II) and Pb(II): speciation modeling of metal-citric acid complexes, J. Hazard. Mater., 155 (2008) 424–432.

[28] A. Idris, E. Misran, N. Hassan, A.A. Jalil, C.E. Seng, Modifed PVA-alginate encapsulated photocatalyst ferro photo gels for Cr (VI) reduction, J. Hazard. Mater., 227–228 (2012) 309–316.

[29] F. Qin, R. Wang, G. Li, F. Tian, H. Zhao, R. Chen, Highly efficient photocatalytic reduction of Cr(VI) by bismuth hollow nanospheres, Catal. Comm., 42 (2013) 14–19.

[30] R. Qiu, D. Zhang, Z. Diao, X. Haung, C. He, J. Morel, Y. Xiong, Visible light induced photocatalytic reduction of Cr (VI) over polymer-sensitized TiO_2 and its synergism with phenol oxidation, Water Res., 46 (2012) 2299–2306.

[31] Y. Guo, X. Lou, D. Xiao, L. Xu, Z. Wang, J. Liu, Sequential reduction-oxidation for photocatalytic degradation of tetrabromobisphenol A: kinetics and intermediates, J. Hazard. Mater., 241–242 (2012) 301–306.

[32] U.D. Patel, J.P. Ruparelia, M.U. Patel, Electrocoagulation treatment of simulated floor-wash containing reactive black 5 using iron sacrificial anode, J. Hazard. Mater., 197 (2011) 128–136.

[33] J. Libra, M. Borchert, L. Vigelahn, T. Storm, Two stage biological treatment of a diazo reactive textile dye and the fate of the dye metabolites, Chemosphere, 56 (2004) 167–180.

[34] C.G. Hatchard, C.A. Parker, A new sensitive chemical actinometer. II. Potassium ferrioxalate as a standard chemical actinometer, Proc. R. Soc. London Ser. A, 235 (1956) 518–536.

[35] M. Montalti, A. Credi, L. Prodi, M.T. Gandolfi, Handbook of Photochemistry, third ed., CRC Press, 2006.

[36] S. Popli, U. Patel, Mechanistic aspects of electro-catalytic reduction of reactive black 5 dye in a divided cell in the presence of silver nano-particles, Sep. Purif. Technol., 179 (2017) 494–503.

[37] R. Patel, S. Suresh, Decolourization of azo dyes using magnesium-palladium system, J. Hazard. Mater., 137 (2006) 1729–1741.

[38] S. Ahmed, M.G. Rasul, R. Brown, M.A. Habib, Influence of parameters on the heterogeneous photocatalytic degradation of pesticides and phenolic contaminants in wastewater: a short review, J. Environ. Manage., 92 (2011) 311–330.

[39] U. Gaya, A. Abdullah, Heterogeneous photocatalytic degradation of organic contaminants over titanium dioxide: a review of fundamentals, process and problems, J. Photochem. Photobiol. C., 9 (2008) 1–12.

[40] X. Gu, S. Lu, X. Fu, Z. Qiu, X. Guo, Carbon dioxide radical anion-based $UV/S_2O_8^{-2}/HCOOH$ reductive process for carbon tetrachloride degradation in aqueous solution, Sep. Purif. Technol., 172 (2017) 211–216.

[41] M. Berkovic, M.C. Gonzalez, N. Russo, M.C. Michelini, R.P. Diez, D.O. Martire, Reduction of mercury(II) by the carbon dioxide radical anion: a theoretical and experimental investigation, J. Phys. Chem., 114 (2010) 12845–12850.

[42] A.V. Rupa, D. Manikandan, D. Divakar, S. Revathi, M.E.L. Preethi, K. Shanthi, T. Sivakumar, Photocatalytic degradation of tatrazine dye using TiO2 catalyst: salt effect and kinetic studies, Indian J. Chem. Technol., 14 (2007) 71–78.

[43] R. Comparelli, E. Fannizza, L.M. Curri, I P. Cozzol, G. Mascolo, R. Passino, Photocatalytic degradation of azo dyes by organic-capped anatase TiO_2 nanocrystals immobilized on to substrates. Appl. Catal. B: Environ., 55 (2005) 81–91.

[44] C.C. Chen, C.S. Lu, Y.C. Chung, J.L. Jan, UV light induced photodegradation of malachite green on TiO_2 nanoparticles, J. Hazard. Mater., 141 (2007) 520–528.

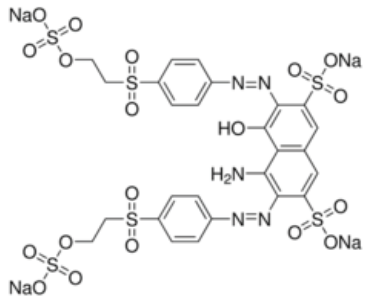## Supplementary information

Table S1
Properties of RB5

Chemical structure	
Chemical class	Diazo
Chemical name	2,7-Naphthalenedisulphonic acid, 4-amino-5-hydroxy-3,6-bis(4-((2-(sulphooxy)ethyl)sulphonyl)phenyl) azo)-tetrasodium salt
Molecular weight	991.8 (g Mol^{-1})
λ_{max} (nm)	595
C.I number	20,505
Supplier	Astron Chemicals, Naroda

Table S2
Physicochemical characteristics of P25 (TiO_2) (source: Evonik Industries)

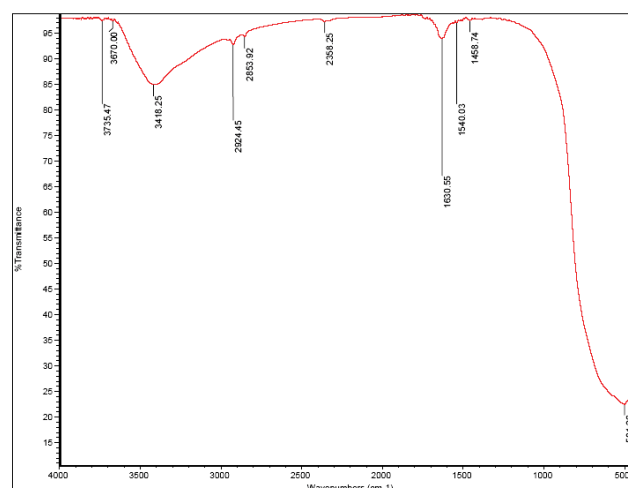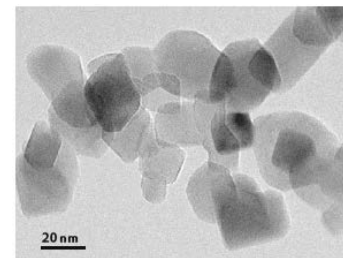|	
Specific surface area (BET)	$50 \pm 15 \ m^2 \ g^{-1}$
TiO_2 content	>99.5 wt%
pH (in 4% dispersion)	3.5–4.5
TEM image of P25	

Fig. S1. FTIR of TiO_2 (P25).